Nanofiltration-enhanced solvent extraction of scandium from TiO_2 acid waste

S. HEDWIG [a,b,†], B. YAGMURLU[c,d,†], D. HUANG[e], O. VON ARX[b], C. DITTRICH[d], E. C. CONSTABLE[b], B. FRIEDRICH[c], M. LENZ [a,f*]

[a] FHNW, Institute for Ecopreneurship, Hofackerstrasse 30, 4132, Muttenz, Switzerland
[b] University of Basel, Department of Chemistry, Mattenstrasse 24a, 4058, Basel, Switzerland
[c] RWTH Aachen University, Department of Process Metallurgy and Metal Recycling, Intzestr. 3, 52056 Aachen, Germany
[d]MEAB Chemie Technik GmbH, 52068 Aachen, Germany
[e]State Key Laboratory of Pollution Control and Resource Reuse, School of the Environment, Nanjing University, Nanjing 210023, Jiangsu Province, PR China
[f]Wageningen University,Sub-Department of Environmental Technology, Bornse Weilanden 9, 6700 AA, Wageningen, The Netherlands

† S.H. and B.Y. contributed equally to this paper.

* Corresponding author, contact: markus1.lenz@wur.nl, Phone: +41 61 228 5686

Abstract

Scandium is a critical raw material with a technological potential to reduce transportation costs and CO_2 emissions. However, global supply and market adoption are crucially impaired by the lack of high-grade Sc ores and recovery strategies. A tandem nanofiltration solvent extraction route is demonstrated to enable effective Sc recovery from real-world acid waste from the chloride TiO_2 production route. The process involving several filtration stages, solvent extraction and precipitation was optimized, ultimately producing >97 % pure $(NH_4)_3ScF_6$.

Keywords: advanced membrane filtration, hydrometallurgy, element recovery, critical raw materials, waste valorisation

Introduction

The intensifying climate crisis demands the transition of society to alternative technologies that can reduce anthropogenic greenhouse emissions to an environmentally acceptable level. The rare earth element (REE) scandium (Sc) offers opportunities for "greening" the energy and transportation industries. For example, solid oxide fuel cells containing Sc can economically produce electricity from hydrogen and Sc is the most efficient dopant for aluminum alloys, allowing the production of ultra-light car bodies.[1,2] Minute amounts of Sc are sufficient for making aircraft Al alloys weldable and 3D printable, with up to 20% weight-saving for future aircraft construction.[3] However, Sc has not been widely adopted by the industry due to limited market availability and astronomical prices (Sc_2O_3: 2'200 USD kg^{-1} in 2021).[4] Suppliers face a number of challenges with regard to Sc: reluctant customers, technologically demanding production processes and shortages of high-quality Sc ores. Due to its (potential) economic importance, which is impeded by a pronounced supply risk, Sc has been classified as a critical raw material (CRM) by the European Commission since 2017.[5,6] The European CRM initiative seeks for measures to remove supply bottlenecks for important commodities. One important strategy is to untap so far unused sources, such as industrial wastes. Although Sc rarely occurs naturally in concentrated ores, it is rather abundant in the Earth's crust (Sc: 22 ppm; Pb: 14 ppm). Overall, Sc is present in hundreds of commercial minerals and can be found in waste streams of mineral industrial processes.[7–9] White pigment (TiO_2) has a global production volume of 8,000,000 $t \cdot a^{-1}$ [10,11] with about half of the TiO_2 being produced by chloride route[12] in which TiO_2-rich ore is digested at high temperatures with elemental chlorine and coke. Volatile $TiCl_4$ is generated and can be condensed from the off-gases of the process. Afterwards, $TiCl_4$ is converted to pure TiO_2 and Cl_2, the latter being recycled. Chlorides of accompanying metals enter the scrubbing water, which eventually turns into a semi-concentrated HCl slurry containing unreacted ore, coal particles and numerous dissolved metals.[13,14] Among these, Sc is in the hundred ppm range, making TiO_2 acid waste a promising Sc resource.[3]

Solvent extraction (SX) is the most commonly used technique to separate and concentrate Sc from aqueous solutions.[7,15–20] The commonest extractants are organophosphorus compounds, such as di-(2-ethylhexyl)phosphoric acid (D2EHPA).[7,15–19] Nevertheless, extraction of trace Sc from complex aqueous media remains technically challenging, requiring high aqueous to organic phase ratios, with the higher costs and emissions associated with large process volumes. In addition, co-extraction of impurities (e.g. Fe, Ti, Zr, Th, U, etc.) reduces the loading capacity and selectivity of the system and directly affects the final purity of the product.[2,21–23] Therefore, strategies for pre-concentration of Sc upstream to SX and reduction of impurities are urgently sought.

One possibility could involve membrane-based technologies such as nanofiltration (NF), which rely on other separation principles than SX.[3] NF membranes bear pores of 0.2-2 nm, corresponding to a molecular weight cut-off (MWCO) of 200 - 1000 Da. Separation of solutes during NF is based on size as well as electrostatic interactions in the case of dissolved ions. Typically, multivalent ions show high retention in NF, while monovalent species easily permeate. Recently, Remmen et al. demonstrated the potential of NF for Sc recovery from TiO_2 acid waste.[3] However, only diluted acid waste was tested and downstream processing was not considered.

Therefore, our study investigated the process engineering needed for Sc recovery from TiO_2 waste, using NF combined with SX, with a view to real-world future implementation. NF was examined using commercial membranes under relevant operating conditions, such as high pressure and with undiluted acid waste. A variety of commercially available acid-resistant NF membranes was tested to account for differences between fabrications and manufacturers. Eventually, NF was used to produce a Sc concentrate from the acid waste.

Sc SX was examined for both the acid waste and the NF concentrate. In this context, the benefits and limits of upstream NF prior to SX were investigated. Effects such as changes in co-extraction, Sc yield, need for post-treatment and plant dimensioning were considered, each being difficult to predict in advance. Ultimately, the overall process was evaluated in regard of implementation possibility for TiO_2 manufacturing via the chloride route.

Materials and Methods

Chemicals and materials

Acid waste was provided from a TiO_2 producer located in the Netherlands. All aqueous solutions were prepared using ultrapure water (>18 MΩ; Barnstead Smart2Pure water purification system, ThermoFisher Scientific, Switzerland). For pH adjustment NaOH solution (30 wt%) was used together with a pH-meter (inoLab Multi 9310 IDS, WTW, Germany). Suspended solids were removed by microfiltration using: 1) vacuum filtration in combination with glass fibre filters (0.4 µm, MN GF-5, Macherey-Nagel, Germany) or 2) decantation and gravity filtration with filtration bags (1 µm, Eurowater, Germany). Residual suspended particles were removed by ultrafiltration (MWCO 150 kDa, UP150, Microdyn-Nadir, Germany) (see 2.4).

Analytical methods

QqQ-ICP-MS

Samples were diluted with nitric acid (3%), using an autodilution system (Simprep, Teledyne Cetac Technologies, USA). Samples were analysed using triple quadrupole inductively coupled plasma mass spectrometry (QqQ-ICP-MS) as previously described.[3] The analysis was performed on an 8800 QqQ-ICP-MS system (Agilent, Basel, Switzerland) using general purpose operational settings. Quantification was performed via multi-element standards (0-50 ppb, seven points). To account for matrix effects ^{103}Rh was used as the internal standard. To quantify $^{23}Na^+$, $^{52}Cr^+$, $^{55}Mn^+$, $^{56}Fe^+$, $^{60}Ni^+$, $^{66}Zn^+$, $^{89}Y^+$, $^{137}Ba^+$, $^{139}La^+$, $^{140}Ce^+$, $^{141}Pr^+$, $^{146}Nd^+$, $^{147}Sm^+$, $^{153}Eu^+$, $^{157}Gd^+$, $^{159}Tb^+$, $^{163}Dy^+$, $^{165}Ho^+$, $^{166}Er^+$, $^{169}Tm^+$, $^{172}Yb^+$, $^{208}Pb^+$, $^{232}Th^+$ and $^{238}U^+$ the ICP-MS was operated in single quad mode using helium as a collision gas, whereas $^{24}Mg^+$, $^{27}Al^+$, $^{39}K^+$, $^{45}Sc^+$, $^{47}Ti^+$, $^{51}V^+$, and $^{90}Zr^+$ were measured in triple quad mass-shift mode using O_2 as a reaction gas. $^{7}Li^+$ concentration was determined using no-gas single quad mode.

Dead-end NF

For dead-end NF a HP4750 stirred cell (Sterlitech, USA, scheme available in SI) was used. Flat sheet membranes (Table S1, SI) were cut into circular shapes and immersed for >20 h in ultrapure water. Afterwards, the membranes were inserted into the cell with the active side (14.6 cm^2) oriented toward the feed solution (100 mL per experiment). The cell was closed and the pressure was adjusted to 35 bar under continuous stirring (300 rpm). Unless otherwise described, filtration was carried out until 30 % permeate was recovered (determined by weight).

Cross-flow filtration

For cross-flow filtration (UF and NF) a modular filtration unit (MaxiMem, PS Prozesstechnik, Switzerland) was used (P&I diagram available in SI). Experiments with flat sheet membranes (active area: 200 cm^2) were conducted at a cross-flow flux of 5 L min^{-1} and a temperature of 25 °C. Spiral wound elements (1812 type: 1.8" diameter, 12" length, 31 mil spacer, 0.32 m^2 active area) were used at a cross-flow flux of 10 L min^{-1} and a temperature of 25 °C. Ultrafiltration (UF) was conducted isobarically at 10 bar under flat sheet conditions. Prior to use, NF membranes were compacted at 10 bar over-night using ultrapure water.

SX

Solvent extraction tests were conducted in a glass beaker with a phase ratio of 1 (50 mL : 50 mL). Each organic phase was contacted with untreated acid waste and NF concentrate for 15 minutes to reach the equilibrium under mild stirring at room temperature. The selected organic phase was loaded with a phase ratio (volume of aqueous phase: volume of organic phase) of 7 for investigations on scrubbing and stripping behaviour. For investigation of loading and scrubbing dependency on Fe valency in the NF concentrate, iron metal (1.5 g L^{-1}) was added to reduce any Fe^{3+} to Fe^{2+}.

For scrubbing tests, HCl (37%, laboratory grade) was diluted with ultrapure water to the desired concentrations. Stripping solutions were prepared using reagent grade NH_4F. Extractants (D2EHPA, Cyanex 923, N1923 and tri-n-butyl phosphate (TBP)) were diluted with dearomatized kerosene (Exxsol D80, ExxonMobile, Germany). Aqueous and re-extraction solutions of the organic phases were sampled for the efficiency calculations.

The distribution ratio and the selectivity of the organic extractants are calculated according to the following equation:

$$D_x = \frac{C_x^{Org}}{C_x^{Aq}} \text{ and } \alpha_{x/y} = \frac{D_x}{D_y} \quad (1)$$

where; D_x is the distribution coefficient of element X, C_x is the concentration of element X in aqueous/organic phase, α is the extraction selectivity.

Results & Discussion

pH-adjustment / preparation of NF feed

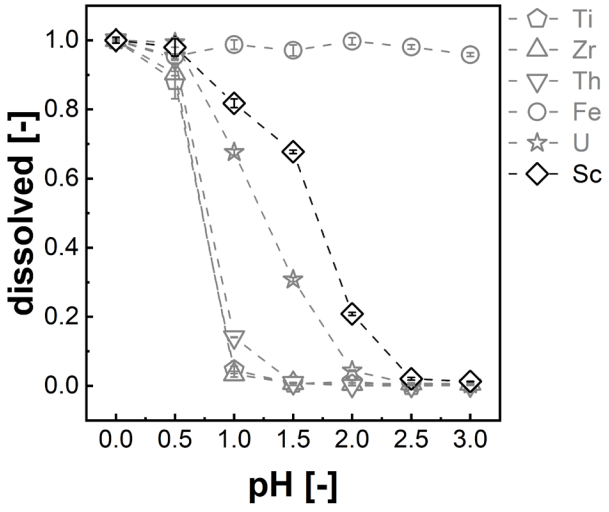

Figure 1: Dissolved elements in the acid waste during neutralisation with NaOH.

The acidic waste from the European TiO_2 production site contained suspended solids (mainly overblown coke and unprocessed ore) and numerous elements in widely varying concentrations. Some of the elements present were known to be problematic for Sc recovery via SX (e.g. Ti, Zr)

or potentially hazardous to health and safety (naturally occurring radioactive material, NORM).[7] Ti can be retained in the solution or scrubbed out of the extractant during SX of the waste from the alternative sulfuric acid TiO_2 production process by adding H_2O_2 to facilitate formation of Ti peroxo sulfate complexes[16] although, this is not possible in the chlorine process in which Ti must be removed before SX.

Excellent separation of Sc from Ti, Zr and Th was achieved at pH 1 to 1.5 (Figure 1). Most of the Sc (82 ± 1% at pH 1; 68 ± 1% at pH 1.5) remained in solution, whilst the other metals precipitated quantitatively (>99%). Adjusting the pH to 1.5 was considered as the best option, as the majority (69 ± 1%) of U also precipitated (Figure 1).

In general, Sc precipitation started at pH >1 and was completed at pH 2.5. For Ti, Zr and Th a steep drop in solubility was observed between pH 0.5 and 1 (Figure 1). Further, U precipitated slightly faster than Sc, starting at pH <1 and being >95% precipitated by pH 2 (Figure 1). In contrast, Fe remained completely dissolved within the range of pH 0 to 3 (Figure 1). The high solubility of Fe indicated the predominant presence of ferrous iron instead of ferric iron[24], as the latter precipitates at pH ≥3.

After pH adjustment, element concentrations in the supernatant were monitored over two weeks. Concentrations were mostly stable over time at different pH values, except near the inflection point of precipitation, where no plateau was reached even after two weeks. There, concentrations increased over time, presumably as a correction of over-precipitation due to local supersaturation.[25] At a pH of 1.5, an equilibration time of 48 hours after NaOH addition was found sufficient.

During S/L separation of the slurry (pH = 1.5), the precipitated hydroxides and oxides were only filtered with difficulty. With filter bags (1 µm sieve size), the filtrate was still turbid, whilst 0.4 µm filters rapidly clogged. The best procedure involved sedimentation of the precipitate (≈48 h) followed by decantation and bag filtration to give a clear solution. The solid fraction (approx. 32% v/v) was a moist gel.

Following microfiltration, residual particles were removed by UF to prevent scaling in subsequent processing. The microfiltrate was easily filterable, with losses determined by the dead volume of

the filtration unit (≈200 mL). The UF permeate, obtained after the pre-treatment, is subsequently referred to as NF feed.

Only few studies of the precipitation behaviour of Sc and other elements contained in the acid waste of the TiO_2 chloride route have been reported. Most recently, Remmen et al. described precipitation trends at pH of 1.5 for different elements in the waste.[3] The precipitation trends at pH 1.5 presented here conform with those previously reported.[3] However, in our system more precipitation was observed (Sc: ~30%, Th: >99% and U: ~70% (here) vs. Sc: ~20%, Th: 80%, U: 40% (Remmen et al.)).[3] We assume this arises from the removal of microparticles by UF. Otherwise, pH values of incipient precipitation reported were extremely low for various elements compared to other literature.[26–29] Precipitation of Th and U is reported to occur between pH 5-7 from chloride media (1-2 for Th from sulfate media).[26] Sc reportedly precipitated at pH ≥3 in HCl.[29] Presumably, the high concentrations of Ti and Zr, whose hydroxides are known to be barely soluble even at a pH of <2, result in co-precipitation.[27]

Overall, the results show that the precipitation of elements in complex real solutions can deviate greatly from findings in model solutions. Although precipitation rates and solubility products are known for the pure compounds, effects such as sorption/coprecipitation and kinetic limitations in complex mixtures make ab initio predictions of behaviour very difficult, making extensive testing inevitable when developing processes based on secondary resources.

NF-membrane screening

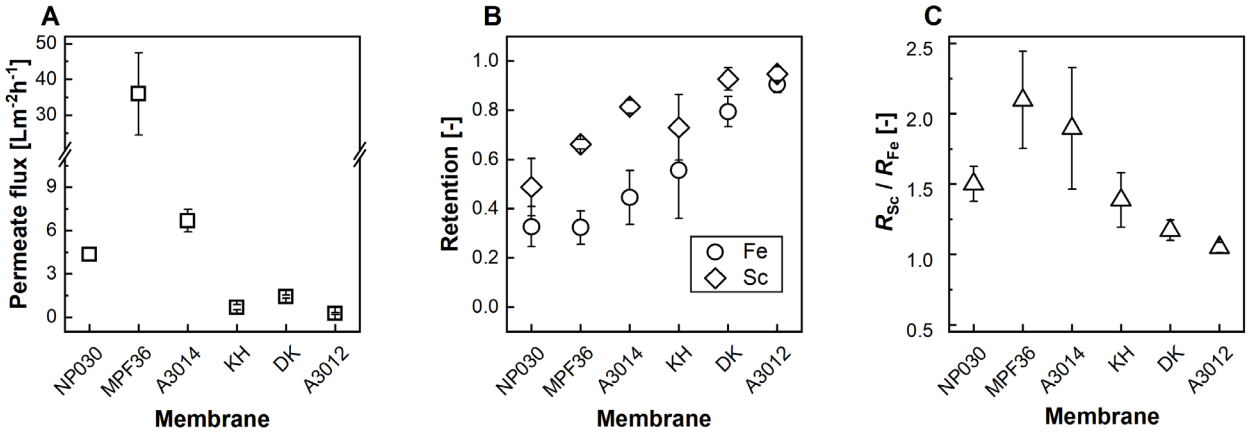

Figure 2: Permeate flux (A), element retention (B) and quotient of Sc over Fe retention (C) (dead-end filtration at 35 bar and 30 % permeate recovery).

Six potential NF-membrane candidates were compared in terms of: 1) permeate flux (Figure 2A), 2) element retention (mainly R_{Sc} and R_{Fe}; Figure 2B) and 3) Sc selectivity (expressed through R_{Sc} divided by R_{Fe}; Figure 2C) during filtration of the NF feed. The membrane showing the best performance of high permeate flux, and high R_{Sc}, while being permeable for competing elements, was A3014, with a permeate flux of 6.7 ±0.8 $Lm^{-2}h^{-1}$, an R_{Sc} of 0.81 ± 0.03 and a Sc over Fe selectivity of 1.9 ±0.4.

The tested membranes had permeate fluxes ranging from 0.25 $Lm^{-2}h^{-1}$ to 35 $Lm^{-2}h^{-1}$, in the sequence A3012 < KH < DK < NP030 < A3014 < MPF36 (Figure 2A), largely consistent with the MWCO reported by the manufacturers (Table S1, SI), with tighter membranes (A3012, DK, KH) showing lower fluxes.

Sc retentions were between 0.49 – 0.95, in the order NP030 < MPF36 < KH < A3014 < DK < A3012 (Figure 2B). For Fe, retentions in the range of 0.32 - 0.90 were observed, following the order MPF36 ≈ NP030 < AMS3014 < KH < DK < A3012 (Figure 2B). Lastly in terms of Sc over Fe selectivity, a range of 1 (no selectivity) to 2 was found, following the order A3012 < DK < KH < NP030 < A3014 < MPF36 (Figure 2C).

While the MWCO were found to be helpful in explaining the trends, there were also exceptions, e.g. the loosest membrane (MPF36, MWCO: 1000 Da) showed the highest flux but not the lowest Sc retention. Instead, the NP030 (MWCO: 500 Da) retained the least Sc, while Fe retention appeared similar to the MPF36. The NP030 showed also a lower flux than the A3014 (MWCO: 400 Da), although being potentially looser.

Low element retention has already been reported for the NP030. Kose Mutlu et al. tested NP030 and the DK for REE recovery from fly ash leachate at low pH.[30] REE retentions were some eight times lower for NP030 in comparison to DK[30] and pH-dependent zeta-potential measurements revealed considerably higher positive surface charges for DK, than for the polyether sulfone membrane NP030.[30] Hence, a potential Donnan rejection mechanism was less pronounced and element retention lower for NP030 than for other membranes.

For NF-based Sc recovery, only MPF36 and A3014 were suitable, as both exhibited good Sc over Fe selectivity and sufficient permeate fluxes. Of the two potential candidates, A3014 was selected for further process development, as a high R_{Sc}, crucial for low Sc losses, was considered more important than high permeate flux. However, MPF36 may represent an interesting choice, when yields are less important than filtration time and operation costs.

Remmen et al. developed layer-by-layer (LbL) assembled NF membranes, which showed a R_{Sc} of up to 0.60 compared to a R_{Fe} of >0.05 and high permeate flux (up to 28 $Lm^{-2}h^{-1}$) at just 5 bar.[3] Aside from NP030, all commercial membranes had higher R_{Sc}, but also higher R_{Fe} values. Therefore, more Sc could be recovered with commercial membranes, but at lower selectivity reaching maximally two times higher R_{Sc} (0.66 and 0.81) than R_{Fe} (0.32 and 0.44) for MPF36 and A3014, respectively. Further, the permeate fluxes were considerably lower compared to LbL membranes: 35 bar pressure were necessary for the MPF36 to reach 36 $Lm^{-2}h^{-1}$, while the second fastest membrane (A3014) reached only ~7 $Lm^{-2}h^{-1}$. However, the test conditions differed to those of Remmen et al., where the acid waste was diluted (1:5).[3] With the higher initial concentration of the feed, a correspondingly higher osmotic pressure had to be overcome and a higher operational pressure was inevitable.

NF process for acid waste concentration

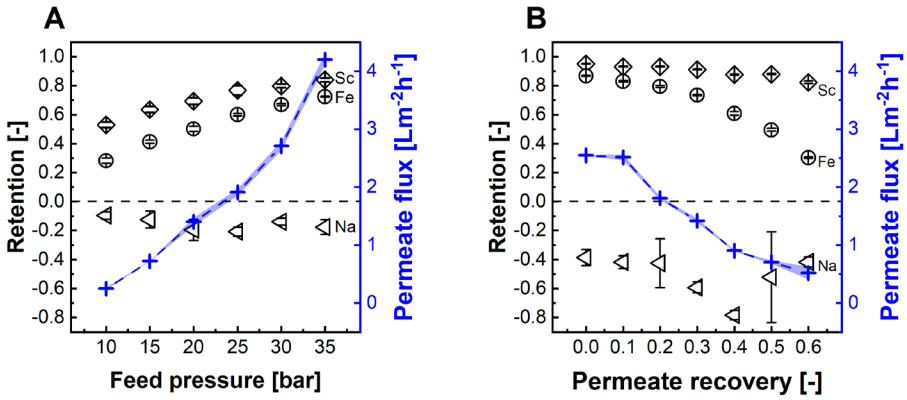

Figure 3: Element retention and permeate flux against the feed pressure at 0% permeate recovery (A) and element retention and permeate flux against the permeate recovery rate at 35 bar (B).

In cross-flow filtration mode with A3014, 35 bar (maximum feed pressure) was optimal in regard to permeate flux (4.2 ±0.1 $Lm^{-2}h^{-1}$) and R_{Sc} (0.84 ±0.01). For Sc selectivity, 1.2 times higher R_{Sc} than R_{Fe} was observed.

Increasing the feed pressure led to almost linear increase of the permeate flux from 0.25 ±0.02 $Lm^{-2}h^{-1}$ (10 bar) to 4.2 ±0.1 $Lm^{-2}h^{-1}$ (35 bar; Figure 3A). At the same time, R_{Sc} improved from 0.53 ±0.02 (10 bar) to 0.84 ±0.01 (35 bar; Figure 3A). In comparison, R_{Fe} started at 0.28 ±0.02 (10 bar) and rose to 0.72 ±0.01 (35 bar). Since R_{Fe} increased faster than R_{Sc}, the selectivity of Sc over Fe decreased from 1.9 (10 bar) to 1.2 (35 bar). In comparison to Sc and Fe, monovalent cations, such as Na^+, were well permeable, indicated by negative retentions throughout the experiments (Figure 3A). Element retentions rose with higher feed pressure due to the subordinate role of diffusive salt transport with simultaneous increase in water permeation.[31]

With regard to R_{Fe}, a discrepancy between crossflow (0.72) and dead end (0.44) filtration was observed, while R_{Sc} was similar (~0.8) in both cases. Therefore, Sc over Fe selectivity was lower during crossflow tests. This is probably due to better compaction when using the cross-flow setup, explaining the higher retentions but also lower permeate flow in these tests.[32] On the other hand, higher concentration polarisation during dead-end filtration conjunct to stronger electrostatic repulsion for Sc^{3+} than for Fe^{2+} might have led to the deterioration of R_{Fe} while being less important for R_{Sc}.[3]

In terms of energy consumption, maintaining the same crossflow rate of 10 $Lmin^{-1}$ at 35 bar required about 2.5 times more energy than at 10 bar.[33] However, the permeate flow at 35 bar increased in comparison 17 times, shortening the operation time and compensating the higher energy consumption at elevated pump load. Therefore, in this case concentrating can be considered more energy efficient at higher pressure.

Ultimately, from 2.0 L NF feed, 0.8 L NF concentrate was produced. Overall, 84 ±3 % of the Sc and 58 ±2 % of the Fe remained in solution (Table 1). The permeate recovery was stopped at around 60 % due to a low permeate flux (0.5 $Lm^{-2}h^{-1}$) decreased R_{Sc} (0.12) and a low residual concentrate volume, being insufficient to maintain a crossflow rate of 10 L min^{-1}.

The permeate flux decreased gradually from 2.5 ±0.1 $Lm^{-2}h^{-1}$ to 0.5 ±0.1 $Lm^{-2}h^{-1}$ (Figure 3B). In terms of element retentions, higher values were found than in the previous experiments. R_{Sc} decreased from 0.95 ±0.01 to 0.82 ±0.01 and Fe became notably more permeable with increasing concentration, with R_{Fe} starting at 0.87 ±0.01 and decreasing to 0.30 ±0.01 at 60 % permeate recovery. Therefore, the Sc over Fe selectivity improved from 1.1 to 2.7. Representative of monovalent ions, Na^+ showed very high permeability throughout the experiment, permeating against its concentration gradient (R_{Na} < -0.3).

During concentration, permeate fluxes and element retentions decreased due to the osmotic pressure increase, as reported before.[3] Interestingly, the Sc retention was less affected than e.g. the Fe retention. It is assumed that this was caused by concentration polarisation, being proportional to element feed concentration, and becoming even more prevalent as filtration progressed and concentrations increased.[34] Permeability, however is expected to be lower for Sc^{3+} than for Fe^{2+}, due to stronger Donnan exclusion. Hence, NF became more selective for Sc with ongoing progress of the operation.

Table 1: Volumes and elemental concentrations for different streams during the production NF concentrate and elemental NF yields and concentration ratios for comparison of NF concentrate with NF feed and initial waste.

		Initial waste	Microfiltrate	NF feed	NF concentrate	NF Yield	concentrate / initial waste	concentrate / NF feed
Volume	**[L]**	3.2	2.2	2.0	0.8		0.24	0.37
Sc	**[mg L^{-1}]**	41.1 ± 0.1	33.3 ± 0.5	28.9 ± 0.5	61 ± 2	0.84 ±0.03	1.5	2.1
Ti	**[mg L^{-1}]**	4540 ± 10	28.5 ± 0.6	5.1 ± 0.2	8.1 ± 0.4	0.64 ±0.04	0.002	1.6
Zr	**[mg L^{-1}]**	1170 ± 20	8.0 ± 0.3	0.12 ± 0.03	0.19 ± 0.02	0.63 ±0.17	0.0002	1.6
Al	**[mg L^{-1}]**	1730 ± 10	1611 ± 30	1430 ± 11	2950 ± 70	0.83 ±0.02	1.7	2.1
Fe	**[mg L^{-1}]**	17600 ± 200	17100 ± 100	15800 ± 200	23100 ± 600	0.58 ±0.02	1.3	1.5
Th	**[mg L^{-1}]**	79 ± 1	5.8 ± 0.2	2.9 ± 0.1	5.4 ± 0.01	0.74 ±0.03	0.07	1.9
U	**[mg L^{-1}]**	13.9 ± 0.2	0.29 ± 0.01	0.09 ± 0.01	0.10 ± 0.01	0.44 ±0.07	0.006	0.9
V	**[mg L^{-1}]**	1070 ± 20	930 ± 30	840 ± 20	1340 ± 40	0.64 ±0.02	1.3	1.6
Na	**[mg L^{-1}]**	150 ± 30	29000 ± 1000	26000 ± 300	15000 ± 400	0.28 ±0.01	100	0.6
Mn	**[mg L^{-1}]**	4600 ± 200	4600 ± 100	4400 ± 100	5500 ± 200	0.5 ±0.02	1.2	1.3

Solvent Extraction Behaviour

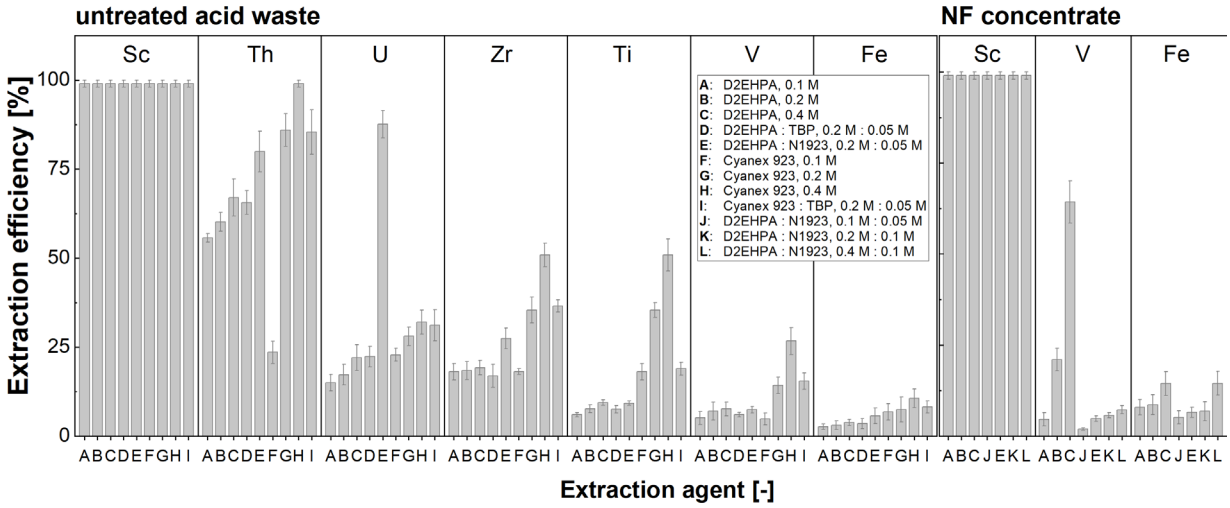

Figure 4: Organic screening for the optimization of the loading behaviour both from untreated acid waste and NF concentrate (impurities with < 10ppm concentration are not included).

Although various studies of the sulfate TiO_2 production route have been reported[16,17,35], limited information is available for SX processes on the chlorine TiO_2 production waste. D2EHPA, Cyanex 923 and synergistic mixtures of these organics worked best to recover Sc selectively from complex solutions from the sulfate process. Therefore, these extractants were tested with various concentrations in D80 kerosene to observe the selectivity, phase separation behaviour and the co-extraction levels of the impurities from untreated acid waste and NF concentrates (Figure 4). All extractants performed similarly in Sc extraction, lowering the Sc concentration to < 1 ppm after extraction in all tests with untreated acid waste (Figure 4). Increasing the D2EHPA concentration did not significantly increase the co-extraction of impurities. While Ti, Zr, V and Fe co-extraction remained stable (Figure 4), extraction of radionuclides increased from 55% to 67% and 15% to 22% for Th and U, respectively. Unlike D2EHPA, increasing Cyanex 923 concentration (to 0.4 $mol \cdot L^{-1}$) resulted in high co-extraction of Th (> 99%), Ti (~50%), Zr (~50%), V (30%) and Fe (10%). No synergistic effect of TBP with these extractants was observed. Co-extraction generally increased with synergistic addition of N1923 to D2EHPA, reaching 85% for Th and 31% for U. Increased NORM extraction was expected, as amines are widely used in commercial solvent extraction of radioactive elements.[36] Even though promising extraction efficiencies were found,

284 the phase separation was problematic in all cases due to high transition metal loading.[37–39] For-
285 mation of an inseparable phase occurred in all extraction trials with slow separation behaviour,
286 predicting high loss of the organic phase and processing problems in a larger scale continuous
287 operation.
288 Extraction tests with the NF concentrate were carried out using the most promising extractants,
289 D2EHPA and synergistic D2EHPA-N1923 couple. Similar to the untreated acid waste, Sc was
290 completely extracted when using NF concentrate. However, high co-extraction was found with
291 D2EHPA as the extractant. This was especially pronounced for higher D2EHPA concentration,
292 reaching 65% for V and 14% for Fe at 0.4 mol·L^{-1} D2EHPA (Figure 4). It was previously reported
293 that addition of N1923 can substantially improve Sc selectivity.[17,40,41] Here, addition of 0.05 mol·L^{-1}
294 efficiently supressed V co-extraction and slightly decreased Fe loading (Figure 4). Sc selectivity
295 over other elements increased during extraction with the synergistic D2EHPA-N1923 mixture (Ta-
296 ble S2, SI). Phases separated rapidly during extraction of the NF concentrate, making the process
297 viable for larger scale operation.
298 Considering the loading capacity, selectivity towards Sc and the phase separation, the best ex-
299 tractant option was identified as 0.2 mol·L^{-1} D2EHPA with 0.05 mol·L^{-1} N1923 in D80 kerosene.
300

301 **Scrubbing**

302 After SX with the selected organic and a phase ratio of 7, Sc was enriched considerably (0.49 g·L^{-1}).
303 Of the major impurities present in the NF concentrate, Fe (6.3 g·L^{-1}) and Al (16 mg·L^{-1}) were
304 found in the organic phase. The trace impurities in NF concentrate, Ti, Zr and Th, were enriched
305 in the organic phase after SX to 32 mg·L^{-1}, 25 mg·L^{-1} and 20 mg·L^{-1}, respectively.
306 HCl was preferred as the scrubbing solution due to strong interaction between Fe and Cl, and
307 avoiding unwanted complex formations from other anions.
308 No Sc was scrubbed out from the organic phase (Table S3, SI). With increasing HCl concentration
309 Ti, Zr, Th, Al removal was only slightly improved, while highest Fe removal (89%) was obtained

with 4 mol·L^{-1} HCl. Therefore, 4 mol·L^{-1} HCl was selected for scrubbing after SX, removing aside from Fe also 72%, 76%, 20% and 56% of Ti, Zr, Th and Al, respectively.

Although the majority of Fe in the NF concentrate was ferrous[24], a fraction oxidized to ferric spontaneously. Presumably, the ferric portion caused high Fe co-extraction, as the affinity of D2EHPA for Fe^{3+} is considerably higher than for Fe^{2+}. In order to suppress Fe co-extraction, iron metal was added to the NF concentrate, reducing Fe^{3+} to Fe^{2+} (equation 2).

$$2\ Fe^{3+} + Fe^{0}_{(s)} \rightarrow 3\ Fe^{2+} \qquad (2)$$

Extraction from three post-treatments for the NF concentrate (original, reduced, reduced & acidified), were compared in terms of Fe co-extraction suppression capability.

Reduction of ferric iron resulted in a sharp drop of the co-extraction values: while 3.3 g·L^{-1} Fe was co-extracted with the original NF concentrate, only 0.36 g·L^{-1} Fe after reduction and 0.17 g·L^{-1} Fe after reduction and acidification were extracted. Thus, reduction & optionally acidification enables complete Fe scrubbing during SX, requiring only few mixer-settler units.

Stripping

Although D2EHPA is a very effective extractant for Sc extraction, its strong bonding characteristics make Sc stripping from the organic phase challenging. Concentrated acids as well as strong alkali solutions have been used for stripping.[42] However, even highly concentrated acids, were relatively unsuccessfully, and concentrated NaOH solutions used instead.[43] Nevertheless, other problems arise from stripping of D2EHPA with NaOH: 1) loss of organic due to solubility of Na-D2EHPA in aqueous solutions, 2) separation issues with 3rd phase formation owing to solubility variations of the extractant in kerosene, 3) immediate precipitation of $Sc(OH)_3$ and clogging of the liquid flow in continuous operation.[38,44,45]

Therefore, NH_4F was selected as the stripping agent due to stable and strong complexation forming $(NH_4)_3ScF_6$. Here, quantitative (>99 %) Sc stripping was achieved (Table 2). The final product contained only traces of impurities, wherefore Sc accounted for ~97 wt-% of the metals in the strip

liquor (Table 2). Residual impurities could be removed via anti-solvent crystallisation, yielding pure $(NH_4)_3ScF_6$.[46] Calcination of this product gives easy access to ScF_3, which can be directly utilized in Al-Sc alloy production.[46] Therefore, high temperature processing to convert $Sc(OH)_3$ into Sc_2O_3 or treatment with gas phase HF to produce ScF_3 can be avoided.

Table 2: Compositions and flows of critical elements through the complete solvent extraction process from NF concentrate to strip liquor.

		Raffinate	Loaded Org.	Scrubbed Org.	Scrubbed Org. (Stage 3)	Stripped Org.	Strip Liquor
Sc	**[mg L^{-1}]**	n.d.	494 ± 7	492 ± 3	491 ± 4	n.d.	1468 ± 31
Ti	**[mg L^{-1}]**	2.7 ± 0.3	31.6 ± 1.8	9.8 ± 0.4	3.4 ± 0.08	n.d.	8.4 ± 1.2
Zr	**[mg L^{-1}]**	n.d.	2.4 ± 0.03	0.4 ± 0.02	0.2 ± 0.01	0.05 ± 0.02	0.5 ± 0.01
Al	**[mg L^{-1}]**	2912 ± 70	24.5 ± 0.8	7.4 ± 0.9	1.1 ± 0.06	0.3 ± 0.03	2.8 ± 0.05
Fe	**[mg L^{-1}]**	22968 ± 600	676 ± 28	38.4 ± 2.2	3.2 ± 0.1	n.d.	9.9 ± 1.0
Th	**[mg L^{-1}]**	1.4 ± 0.1	22 ± 1.1	15.4 ± 0.7	8.6 ± 0.7	1.5 ± 0.05	23.4 ± 2.9
U	**[mg L^{-1}]**	n.d.	0.09 ± 0.01	n.d.	n.d	n.d.	n.d.

Process flow scheme / integration into chloride route

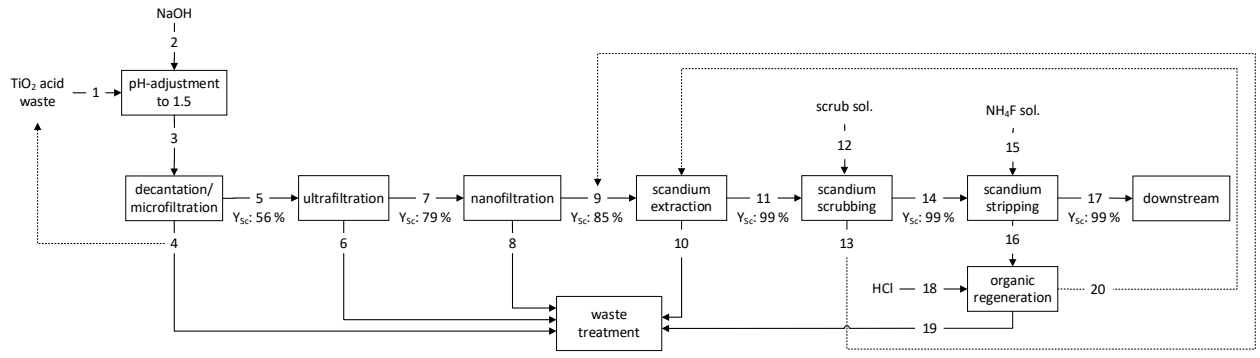

Figure 5: Block flow diagram of the tandem NF-SX process for Sc recovery from TiO_2 acid waste.

The proposed Sc recovery process comprises seven stages (Figure 5). From pH adjustment to NF, only sodium hydroxide, electrical power and re-usable filters/membranes, were required. NaOH, although expensive compared to lime/limestone, was needed to avoid high multivalent

cations concentrations (e.g. Ca^{2+}) which would be enriched during NF due to high retentions, increasing the osmotic pressure of the feed, opposing the feasibility of the filtration. However, in view of the overall process (i.e. Sc recovery conjunct to chloride route TiO_2 production), NaOH might be available from upstream chlorine production via NaCl electrolysis, saving on transportation costs.[47]

In terms of Sc yields, the S/L separation (i.e. MF & UF) brought substantial losses (around 56%). Thus, despite the high yields (82%, four stages) following UF, the overall Sc yield was 36%. However, these could be mitigated by more efficient S/L of the hydroxide sludge, such as by the use of a filter press. Losses during lab-scale UF (stream 6) due to the dead volume of the filtration unit would become negligible on a larger scale. Alternatively, streams 4 and 6 could be redirected into the original acid waste. This would reduce the amount of Sc discharge. Neutralisation followed by S/L separation, is currently used for acid waste treatment after chlorine TiO_2 production. Hence, NF feed could be produced by minor adjustment of the current treatment conditions.

During NF, most of the Sc (85 %) was preserved in the concentrate. The NF permeate (stream 8) is relatively diluted compared to the upstream media and could be re-used as scrubbing water in the gas washer of the TiO_2 production process. This would contribute to a zero liquid discharge approach and would keep NF related Sc losses in the system.

SX downstream to NF allowed for quantitative (99 %) Sc recovery from the concentrate. Due to excellent phase separation, no organic should be in the raffinate (stream 10). This Sc depleted solution could either be returned to the existing TiO_2 waste treatment process or could serve for further element recovery (e.g. V, Mn, other REE). The scrubbing effluent (stream 13) could be reused for acidification of the NF concentrate once Fe^0 was added (Figure S3, SI). Compared to the NF concentrate the throughput of stream 13 was rather low. Hence, combination of 13 and 9 would lead to negligible dilution but allow for waste mitigation and pH adjustment.

After Sc recovery via NF and SX, the Sc depleted solutions could be returned into the existing waste treatment route.

Conclusion

A combination of NF and SX has been applied to recover Sc from acid waste, originating from chloride-route TiO_2 production. The major findings were:

- pH adjustment 1-1.5 preserved Sc dissolved, precipitated challenging impurities (Ti, Zr, Th, U)
- AMS Nanopro A-3014 provided best trade-off between permeate flux, Sc retention & selectivity
- At most effective pressure of 35 bar, 60% of the volume and various bulk impurities (such as ~40% Fe, V, Mn) were removed, while 85% of Sc remained in the concentrate
- A mixture of D2EHPA and N1923 was most selective in SX
- Upstream removal of Ti, Zr, Th, U drastically increased Sc selectivity during SX
- NF prior to SX improved phase separation and reduced process volume
- Addition of Fe^0 suppressed Fe^{3+} coextraction and improved Fe scrubbing
- NH_4F was found as highly efficient stripping agent for Sc (purity >97%)
- Overall Sc recovery was 36% (six stages), which could be improved in the future by more efficient engineering of the MF & UF stages

The proposed process could be integrated into the waste disposal unit of a TiO_2 production plant without drastic plant changes and could be a step towards waste valorisation and effective resource use, enabling the production of a CRM with promising future potential.

Supporting Information

Description and properties of the membranes, schemes of the used filtration units, comparison of Fe loading efficiencies, Sc selectivity over major impurities, impurity scrubbing efficiencies from the loaded D2EHPA+N1923.

Acknowledgements

This project has received funding from the European Union's Horizon 2020 research and innovation programme under grant agreement No. 730105 (SCALE: www.scale-project.eu/). This work was supported by the Swiss State Secretariat for Education, Research and Innovation (SERI) under contract number 16.0155. The opinions expressed and arguments employed herein do not necessarily reflect the official views of the Swiss government. Roman Schäfer and Kirsten Remmen are kindly thanked for their assistance during this study.

References

(1) Ahmad, Z. The properties and application of scandium-reinforced aluminum. *JOM* **2003**, *55* (2), 35–39. DOI: 10.1007/s11837-003-0224-6.

(2) Botelho Junior, A. B.; Espinosa, D.; Vaughan, J.; Tenório, J. Recovery of scandium from various sources: A critical review of the state of the art and future prospects. *Miner. Eng.* **2021**, *172*, 107148. DOI: 10.1016/j.mineng.2021.107148.

(3) Remmen, K.; Schäfer, R.; Hedwig, S.; Wintgens, T.; Wessling, M.; Lenz, M. Layer-by-layer membrane modification allows scandium recovery by nanofiltration. *Environ. Sci.: Water Res. Technol.* **2019**, *5* (10), 1683–1688. DOI: 10.1039/C9EW00509A.

(4) Gambogi, J. *USGS Mineral Commodity Summary: Scandium,* **2022**.

(5) European Commission *On the 2017 list of Critical Raw Materials for the EU*:*COM(2017) 490 final,* **2017**.

(6) European Commission *Critical Raw Materials Resilience: Charting a Path towards Greater Security and Sustainability*:*COM/2020/474 final,* **2020**.

(7) Wang, W.; Pranolo, Y.; Cheng, C. Y. Metallurgical processes for scandium recovery from various resources: A review. *Hydrometallurgy* **2011**, *108* (1-2), 100–108. DOI: 10.1016/j.hydromet.2011.03.001.

(8) Alkan, G.; Yagmurlu, B.; Cakmakoglu, S.; Hertel, T.; Kaya, Ş.; Gronen, L.; Stopic, S.; Friedrich, B. Novel Approach for Enhanced Scandium and Titanium Leaching Efficiency from Bauxite Residue with Suppressed Silica Gel Formation. *Scientific reports* **2018**, *8* (1), 5676. DOI: 10.1038/s41598-018-24077-9. Published Online: Apr. 4, 2018.

(9) Kaya, Ş.; Dittrich, C.; Stopic, S.; Friedrich, B. Concentration and Separation of Scandium from Ni Laterite Ore Processing Streams. *Metals* **2017**, *7* (12), 557. DOI: 10.3390/met7120557.

(10) Gambogi, J. *USGS Minerals Information: Titanium and titanium dioxide,* **2021**.

(11) Zhang, W.; Zhu, Z.; Cheng, C. Y. A literature review of titanium metallurgical processes. *Hydrometallurgy* **2011**, *108* (3-4), 177–188. DOI: 10.1016/j.hydromet.2011.04.005.

(12) Perks, C.; Mudd, G. Titanium, zirconium resources and production: A state of the art literature review. *Ore Geol. Rev.* **2019**, *107*, 629–646. DOI: 10.1016/j.oregeorev.2019.02.025.

(13) Gázquez, M. J.; Bolívar, J. P.; Garcia-Tenorio, R.; Vaca, F. A Review of the Production Cycle of Titanium Dioxide Pigment. *MSA* **2014**, *05* (07), 441–458. DOI: 10.4236/msa.2014.57048.

(14) Yagmurlu, B.; Orberger, B.; Dittrich, C.; Croisé, G.; Scharfenberg, R.; Balomenos, E.; Panias, D.; Mikeli, E.; Maier, C.; Schneider, R.; Friedrich, B.; Dräger, P.; Baumgärtner, F.; Schmitz, M.; Letmathe, P.; Sakkas, K.; Georgopoulos, C.; van den Laan, H. *Sustainable Supply of Scandium for the EU Industries from Liquid Iron Chloride Based TiO_2 Plants*; International Conference on Raw Materials and Circular Economy, **2021**. DOI: 10.3390/materproc2021005086.

(15) Zhou, J.; Ning, S.; Meng, J.; Zhang, S.; Zhang, W.; Wang, S.; Chen, Y.; Wang, X.; Wei, Y. Purification of scandium from concentrate generated from titanium pigments production waste. *Journal of Rare Earths* **2020.** DOI: 10.1016/j.jre.2020.02.008.

(16) Qiu, H.; Wang, M.; Xie, Y.; Song, J.; Huang, T.; Li, X.-M.; He, T. From trace to pure: Recovery of scandium from the waste acid of titanium pigment production by solvent extraction. *Process Safety and Environmental Protection* **2019**, *121*, 118–124. DOI: 10.1016/j.psep.2018.10.027.

(17) Zou, D.; Li, H.; Chen, J.; Li, D. Recovery of scandium from spent sulfuric acid solution in titanium dioxide production using synergistic solvent extraction with D2EHPA and primary amine N1923. *Hydrometallurgy* **2020**, *197*, 105463. DOI: 10.1016/j.hydromet.2020.105463.

(18) Salman, A. D.; Juzsakova, T.; Mohsen, S.; Abdullah, T. A.; Le, P.-C.; Sebestyen, V.; Sluser, B.; Cretescu, I. Scandium Recovery Methods from Mining, Metallurgical Extractive Industries, and Industrial Wastes. *Materials* **2022**, *15* (7), 2376. DOI: 10.3390/ma15072376.

(19) Zhou, J.; Ma, S.; Chen, Y.; Ning, S.; Wei, Y.; Fujita, T. Recovery of scandium from red mud by leaching with titanium white waste acid and solvent extraction with P204. *Hydrometallurgy* **2021**, *204*, 105724. DOI: 10.1016/j.hydromet.2021.105724.

(20) Zhou, J.; Yu, Q.; Huang, Y.; Meng, J.; Chen, Y.; Ning, S.; Wang, X.; Wei, Y.; Yin, X.; Liang, J. Recovery of scandium from white waste acid generated from the titanium sulphate process using solvent extraction with TRPO. *Hydrometallurgy* **2020**, *195*, 105398. DOI: 10.1016/j.hydromet.2020.105398.

(21) Smirnov, A. L.; Titova, S. M.; Rychkov, V. N.; Bunkov, G. M.; Semenishchev, V. S.; Kirillov, E. V.; Poponin, N. N.; Svirsky, I. A. Study of scandium and thorium sorption from uranium leach liquors. *J. Radioanal. Nucl. Chem.* **2017**, *312* (2), 277–283. DOI: 10.1007/s10967-017-5234-x.

(22) Yagmurlu, B.; Alkan, G.; Xakalashe, B.; Schier, C.; Gronen, L.; Koiwa, I.; Dittrich, C.; Friedrich, B. Synthesis of Scandium Phosphate after Peroxide Assisted Leaching of Iron Depleted Bauxite Residue (Red Mud) Slags. *Scientific reports* **2019**, *9* (1), 11803. DOI: 10.1038/s41598-019-48390-z. Published Online: Aug. 14, 2019.

(23) Yagmurlu, B.; Dittrich, C.; Friedrich, B. Precipitation Trends of Scandium in Synthetic Red Mud Solutions with Different Precipitation Agents. *J. Sustain. Metall.* **2017**, *3* (1), 90–98. DOI: 10.1007/s40831-016-0098-9.

(24) European Commission *Reference Document on Best Available Techniques for the Manufacture of Large Volume Inorganic Chemicals - Solids and Others industry*, Seville, Spain, **2007**.

(25) Rene, E. R. *Sustainable Heavy Metal Remediation*:*Volume 1: Principles and Processes*; Springer International Publishing, Cham, **2017**; pp. 101–120.

(26) García, A. C.; Latifi, M.; Amini, A.; Chaouki, J. Separation of Radioactive Elements from Rare Earth Element-Bearing Minerals. *Metals* **2020**, *10* (11), 1524. DOI: 10.3390/met10111524.

(27) Svandova, M.; Raschman, P.; Sucik, G.; Dorakova, A.; Fedorockova, A. Removal of Heavy Metals From Wastewater Using Caustic Calcinated Magnesia **2015**, *21* (3), 247–252. DOI: 10.12776/ams.v21i3.536.

(28) Blais, J. F.; Djedidi, Z.; Cheikh, R. B.; Tyagi, R. D.; Mercier, G. Metals Precipitation from Effluents: Review. *Pract. Period. Hazard. Toxic Radioact. Waste Manage.* **2008**, *12* (3), 135–149. DOI: 10.1061/(ASCE)1090-025X(2008)12:3(135).

(29) Yagmurlu, B.; Dittrich, C.; Friedrich, B. Effect of Aqueous Media on the Recovery of Scandium by Selective Precipitation. *Metals* **2018**, *8* (5), 314. DOI: 10.3390/met8050314.

(30) Kose Mutlu, B.; Cantoni, B.; Turolla, A.; Antonelli, M.; Hsu-Kim, H.; Wiesner, M. R. Application of nanofiltration for Rare Earth Elements recovery from coal fly ash leachate: Performance and cost evaluation. *Chemical Engineering Journal* **2018**, *349*, 309–317. DOI: 10.1016/j.cej.2018.05.080.

(31) Schütte, T.; Niewersch, C.; Wintgens, T.; Yüce, S. Phosphorus recovery from sewage sludge by nanofiltration in diafiltration mode. *Journal of Membrane Science* **2015**, *480*, 74–82. DOI: 10.1016/j.memsci.2015.01.013.

(32) Hussain, Y. A.; Al-Saleh, M. H.; Ar-Ratrout, S. S. The effect of active layer non-uniformity on the flux and compaction of TFC membranes. *Desalination* **2013**, *328*, 17–23. DOI: 10.1016/j.desal.2013.08.008.

(33) Wanner Engineering, Inc. *G03 Series Datasheet*. https://www.hydra-cell.com/ltr2/access.php?file=pdf/G03-Datasheet.pdf, **2021**.

(34) Mdemagh, Y.; Hafiane, A.; Ferjani, E. Characterization and modeling of the polarization phenomenon to describe salt rejection by nanofiltration. *4open* **2018**, *1*, 5. DOI: 10.1051/fopen/2018005.

(35) Lei, Q.; He, D.; Zhou, K.; Zhang, X.; Peng, C.; Chen, W. Separation and recovery of scandium and titanium from red mud leaching liquor through a neutralization precipitation-acid leaching approach. *Journal of Rare Earths* **2021**, *39* (9), 1126–1132. DOI: 10.1016/j.jre.2020.07.030.

(36) Hung, N. T.; Le Thuan, B.; Thanh, T. C.; Watanabe, M.; van Khoai, D.; Thuy, N. T.; Nhuan, H.; Minh, P. Q.; Mai, T. H.; van Tung, N.; Tra, D. T. T.; Jha, M. K.; Lee, J.-Y.; Jyothi, R. K. Separation of thorium and uranium from xenotime leach solutions by solvent extraction using primary and tertiary amines. *Hydrometallurgy* **2020**, *198*, 105506. DOI: 10.1016/j.hydromet.2020.105506.

(37) Gupta, B.; Deep, A.; Malik, P.; Tandon, S. N. Extraction and Separation of Some 3d Transition Metal Ions Using Cyanex 923. *Solvent Extraction and Ion Exchange* **2002**, *20* (1), 81–96. DOI: 10.1081/SEI-100108826.

(38) Yurtov, E. V.; Murashova, N. M. Gels, emulsions, and liquid crystals in extraction systems with Di(2-ethylhexyl)phosphoric acid. *Theor Found Chem Eng* **2007**, *41* (5), 737–742. DOI: 10.1134/S0040579507050508.

(39) Chen, Y.; Ma, S.; Ning, S.; Zhong, Y.; Wang, X.; Fujita, T.; Wei, Y. Highly efficient recovery and purification of scandium from the waste sulfuric acid solution from titanium dioxide production by solvent extraction. *Journal of Environmental Chemical Engineering* **2021**, *9* (5), 106226. DOI: 10.1016/j.jece.2021.106226.

(40) Yagmurlu, B.; Dittrich, C.; Friedrich, B. *Innovative scandium refining processes from secondary raw materials.*; European Scandium Inventory Workshops, **2018**.

(41) Yagmurlu, B.; Dittrich, C.; Davris, P.; Balomenos, E.; Pilichou, A.; Panias, D.; Friedrich, B. *Recovery of scandium from bauxite residue via solvent extraction.*; Proceedings of 3rd International Bauxite Residue Valorisation and Best Practices Conference, **2020**.

(42) Wang, W.; Cheng, C. Y. Separation and purification of scandium by solvent extraction and related technologies: a review. *J. Chem. Technol. Biotechnol.* **2011**, *86* (10), 1237–1246. DOI: 10.1002/jctb.2655.

(43) Wang, W.; Pranolo, Y.; Cheng, C. Y. Recovery of scandium from synthetic red mud leach solutions by solvent extraction with D2EHPA. *Separation and Purification Technology* **2013**, *108*, 96–102. DOI: 10.1016/j.seppur.2013.02.001.

(44) Wang, D.; Li, Y.; Wu, J.; Xu, G. Mechanism of the extractant loss in lanthanide extraction process with saponified organophosphorus acid extraction systems - II: formation of aqueous

aggregates:Mechanism of the extractant loss in lanthanide extraction process with saponified organophosphorus acid extraction systems - II: formation of aqueous aggregates. *Solvent Extraction and Ion Exchange* **1996**, *14* (4), 585–601. DOI: 10.1080/07366299608918358.

(45) Sun, M.; Liu, S.; Zhang, Y.; Liu, M.; Yi, X.; Hu, J. Insights into the saponification process of di(2-ethylhexyl) phosphoric acid extractant: Thermodynamics and structural aspects. *Journal of Molecular Liquids* **2019**, *280*, 252–258. DOI: 10.1016/j.molliq.2019.02.025.

(46) Kaya, Ş.; Peters, E.; Forsberg, K.; Dittrich, C.; Stopic, S.; Friedrich, B. Scandium Recovery from an Ammonium Fluoride Strip Liquor by Anti-Solvent Crystallization. *Metals* **2018**, *8* (10), 767. DOI: 10.3390/met8100767.

(47) Li, K.; Fan, Q.; Chuai, H.; Liu, H.; Zhang, S.; Ma, X. Revisiting Chlor-Alkali Electrolyzers: from Materials to Devices. *Trans. Tianjin Univ.* **2021**, *27* (3), 202–216. DOI: 10.1007/s12209-021-00285-9.

For Table of Contents Use Only

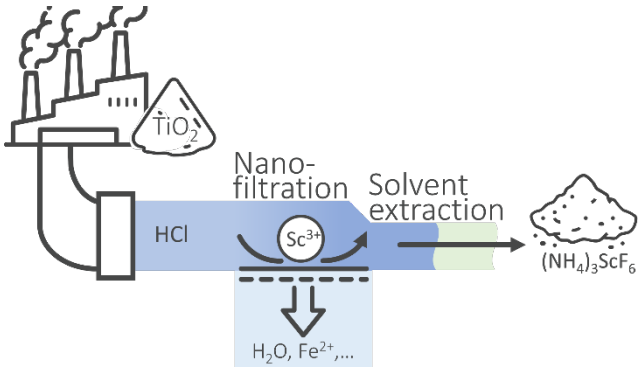

Synopsis: Scandium separation by combination of nanofiltration and solvent extraction; pure $(NH_4)_3ScF_6$ is recovered from TiO_2 production acid waste